USGS
science for a changing world

Prepared in cooperation with the International Joint Commission

A Review of Surface Energy Balance Models for Estimating Actual Evapotranspiration with Remote Sensing at High Spatiotemporal Resolution over Large Extents

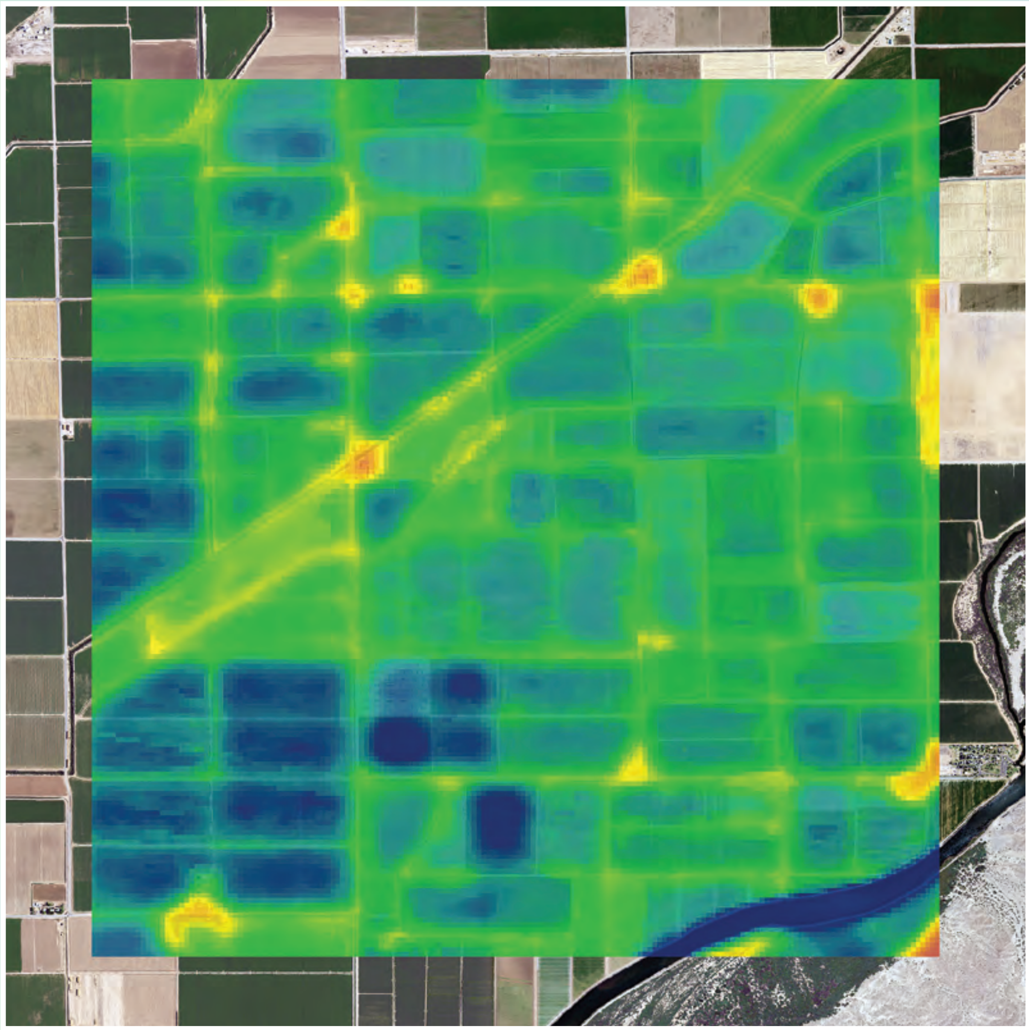

Scientific Investigations Report 2017–5087

U.S. Department of the Interior
U.S. Geological Survey

Cover. Aerial imagery of an irrigation district in southern California along the Colorado River with actual evapotranspiration modeled using Landsat data https://earthexplorer.usgs.gov; https://doi.org/10.5066/F7DF6PDR.

A Review of Surface Energy Balance Models for Estimating Actual Evapotranspiration with Remote Sensing at High Spatiotemporal Resolution over Large Extents

By Ryan R. McShane, Katelyn P. Driscoll, and Roy Sando

Prepared in cooperation with the International Joint Commission

Scientific Investigations Report 2017–5087

U.S. Department of the Interior
U.S. Geological Survey

U.S. Department of the Interior
RYAN K. ZINKE, Secretary

U.S. Geological Survey
William H. Werkheiser, Acting Director

U.S. Geological Survey, Reston, Virginia: 2017

For more information on the USGS—the Federal source for science about the Earth, its natural and living resources, natural hazards, and the environment—visit https://www.usgs.gov or call 1–888–ASK–USGS.

For an overview of USGS information products, including maps, imagery, and publications, visit https://store.usgs.gov.

Suggested citation:
McShane, R.R., Driscoll, K.P., and Sando, Roy, 2017, A review of surface energy balance models for estimating actual evapotranspiration with remote sensing at high spatiotemporal resolution over large extents: U.S. Geological Survey Scientific Investigations Report 2017–5087, 19 p., https://doi.org/10.3133/sir20175087.

ISSN 2328-0328 (online)

Contents

Tables

Conversion Factors

International System of Units to U.S. customary units

Multiply	By	To obtain
	Length	
millimeter (mm)	0.03937	inch (in.)
meter (m)	3.281	foot (ft)
kilometer (km)	0.6214	mile (mi)
	Area	
hectare (ha)	2.471	acre
square kilometer (km^2)	0.3861	square mile (mi^2)
	Volume	
cubic kilometer (km^3)	0.2399	cubic mile (mi^3)
	Flow rate	
millimeter per hour (mm/h)	0.003281	foot per hour (ft/hr)
	Density	
kilogram per cubic meter (kg/m^3)	0.06242	pound per cubic foot (lb/ft^3)
	Energy	
joule (J)	0.0000002	kilowatthour (kWh)

Abbreviations

α	surface albedo
ε_0	broadband surface thermal emissivity
λ	latent heat of vaporization
ρ_{air}	density of air
ρ_w	density of water
ALEXI	Atmosphere-Land Exchange Inverse
ASTER	Advanced Spaceborne Thermal Emission and Reflection Radiometer
C_p	specific heat of air at constant pressure
DEM	digital elevation model
dT	temperature difference between two near-surface heights (temperature gradient)
DTD	Dual Temperature Difference
EF	evaporative fraction
ET	evapotranspiration
ET_0	reference evapotranspiration
ET_a	actual evapotranspiration
ETEML	Enhanced Two-Source Evapotranspiration Model for Land
ET_f	fractional evapotranspiration

$ET_{f(el)}$	fractional evapotranspiration corrected for elevation
$ET_{f(elvi)}$	fractional evapotranspiration corrected for elevation and vegetation index
ET_{inst}	instantaneous actual evapotranspiration
ET_{period}	actual evapotranspiration cumulated over a period
ET_r	reference evapotranspiration
ET_rF	reference evapotranspiration fraction
G	ground heat flux
GDAS	Global Data Assimilation System
H	sensible heat flux
HUC8	8-digit hydrologic unit code
K	Kelvin
K_L	lapse rate in temperature of air moving over the landscape
LAI	leaf area index
LE	latent heat flux
LST	land surface temperature
LST_c	land surface temperature corrected for elevation
METRIC	Mapping Evapotranspiration at High Resolution with Internalized Calibration
MODIS	Moderate Resolution Imaging Spectroradiometer
NDVI	normalized difference vegetation index
NSE	Nash-Sutcliffe efficiency
PRISM	Parameter-Elevation Regressions on Independent Slopes Model
r	correlation coefficient
r^2	coefficient of determination
r_{ah}	aerodynamic resistance between two near-surface heights
RMSE	root mean square error
$R_{L\downarrow}$	incoming longwave radiation
$R_{L\uparrow}$	outgoing longwave radiation
R_n	net radiation
$R_{S\downarrow}$	incoming shortwave radiation
S-SEBI	Simplified Surface Energy Balance Index
SEBAL	Surface Energy Balance Algorithm for Land
SEBS	Surface Energy Balance System
SSEB	Simplified Surface Energy Balance
SSEBelvi	Simplified Surface Energy Balance with correction for elevation and vegetation index
SSEBop	Operational Simplified Surface Energy Balance

T_a	air temperature
T_c	land surface temperature at “cold” reference pixel
T_h	land surface temperature at “hot” reference pixel
T_s	land surface temperature
$T_{s\ datum}$	land surface temperature adjusted to a standard elevation per pixel of the satellite image
TSM	Two-Source Model
TSTIM	Two-Source Time Integrated Model

A Review of Surface Energy Balance Models for Estimating Actual Evapotranspiration with Remote Sensing at High Spatiotemporal Resolution over Large Extents

By Ryan R. McShane, Katelyn P. Driscoll, and Roy Sando

Abstract

Many approaches have been developed for measuring or estimating actual evapotranspiration (ET_a), and research over many years has led to the development of remote sensing methods that are reliably reproducible and effective in estimating ET_a. Several remote sensing methods can be used to estimate ET_a at the high spatial resolution of agricultural fields and the large extent of river basins. More complex remote sensing methods apply an analytical approach to ET_a estimation using physically based models of varied complexity that require a combination of ground-based and remote sensing data, and are grounded in the theory behind the surface energy balance model. This report, funded through cooperation with the International Joint Commission, provides an overview of selected remote sensing methods used for estimating water consumed through ET_a and focuses on Mapping Evapotranspiration at High Resolution with Internalized Calibration (METRIC) and Operational Simplified Surface Energy Balance (SSEBop), two energy balance models for estimating ET_a that are currently applied successfully in the United States. The METRIC model can produce maps of ET_a at high spatial resolution (30 meters using Landsat data) for specific areas smaller than several hundred square kilometers in extent, an improvement in practice over methods used more generally at larger scales. Many studies validating METRIC estimates of ET_a against measurements from lysimeters have shown model accuracies on daily to seasonal time scales ranging from 85 to 95 percent. The METRIC model is accurate, but the greater complexity of METRIC results in greater data requirements, and the internalized calibration of METRIC leads to greater skill required for implementation. In contrast, SSEBop is a simpler model, having reduced data requirements and greater ease of implementation without a substantial loss of accuracy in estimating ET_a. The SSEBop model has been used to produce maps of ET_a over very large extents (the conterminous United States) using lower spatial resolution (1 kilometer) Moderate Resolution Imaging Spectroradiometer (MODIS) data. Model accuracies ranging from 80 to 95 percent on daily to annual time scales have been shown in numerous studies that validated ET_a estimates from SSEBop against eddy covariance measurements. The METRIC and SSEBop models can incorporate low and high spatial resolution data from MODIS and Landsat, but the high spatiotemporal resolution of ET_a estimates using Landsat data over large extents takes immense computing power. Cloud computing is providing an opportunity for processing an increasing amount of geospatial "big data" in a decreasing period of time. For example, Google Earth Engine™ has been used to implement METRIC with automated calibration for regional-scale estimates of ET_a using Landsat data. The U.S. Geological Survey also is using Google Earth Engine™ to implement SSEBop for estimating ET_a in the United States at a continental scale using Landsat data.

Introduction

Consumptive water use refers to water that is evaporated and transpired from soils, vegetation, and open water (collectively called evapotranspiration [ET]); ingested by livestock and humans; or incorporated into crops and other commodities; and that consequently is unavailable for other demands on a water supply (Maupin and others, 2014). Most water consumption is through actual evapotranspiration (ET_a), which is an important component of the water cycle, and it is estimated that about 70 percent of precipitation on land in the United States returns to the atmosphere through ET_a (Carr and others, 1990). In addition, in the United States, more than 80 percent of water consumption is for agriculture (Carr and others, 1990), most of which is from ET_a. Therefore, water resource users and managers have a vested interest in accurately determining consumptive water use, especially when considering the effect of population growth and climate change on water demand and supply (Vörösmarty and others, 2000). Distribution of water resources depends on knowing the volume of water that initially is available for use and knowing how much of that water is consumed, thus making it unavailable for additional uses.

Many approaches have been developed for measuring or estimating ET_a, which constitutes a large fraction of consumptive water use (Allen and others, 2011b). The ET_a at a site can be measured directly using lysimeters (Pruitt and Angus, 1960), eddy covariance flux towers (Swinbank, 1951), or scintillometers (Meijninger and others, 2002); however, using these instruments can involve substantial expense and effort and requires well-trained personnel. The ET_a also can be measured indirectly at a site using evaporation pans (Snyder, 1992) or Bowen ratio stations (Fritschen, 1965). The use of these instruments, although requiring less expense and training than directly measuring ET_a, still entails considerable labor. Additionally, these direct and indirect measurements of ET_a are limited to the sites and times at which they are taken.

A simple technique for estimating ET_a over larger extents and longer time periods involves the use of crop coefficients (Allen and others, 1998). A crop coefficient is a factor that relates ET_a of a plant to that of a reference state by parameterizing several characteristics of the plant and the soil. Crop coefficients have been developed for numerous plant species. This technique can be scaled to larger extents or longer time periods and transferred among sites because crop coefficients are fixed parameters, although a crop type may have several factors depending on the number of growth stages (for example, initial and development). Applying this technique more broadly, however, is difficult because of complications with determining crop types or growth stages from aerial photography or satellite imagery. Furthermore, this technique makes a questionable assumption that local conditions affecting parameters are spatially homogenous. Despite these limitations, the crop coefficient technique is still used worldwide because of its simplicity (Allen, 2000; Allen and others, 2005a).

Remote sensing data have been useful in developing methods for estimating consumptive water use from ET_a that are scalable and transferable, which is important because apportionment of water resources is affected by environmental and economic circumstances differing in extent and spatiotemporal resolution. Research over many years has led to the development of remote sensing methods that are reliably reproducible and effective in estimating ET_a. Since satellites first began collecting data on natural resources in the 1970s, researchers have been developing models to process these data for estimating ET_a (Idso and others, 1975; Jackson and others, 1977). Some remote sensing methods for estimating ET_a are focused at very local scales (Jackson and others, 1977), whereas others are focused at scales ranging from regional or continental (Senay and others, 2013; Singh and Senay, 2016) to global (Mu and others, 2007). These methods also range from simple (Jackson and others, 1977) to complex (Bastiaanssen and others, 1998a; Allen and others, 2007b). Several remote sensing methods can be used to estimate ET_a at the high spatial resolution of agricultural fields and the large extent of river basins—a scale that is useful to water resource managers.

Purpose and Scope

This report, prepared in cooperation with the International Joint Commission, provides an overview of selected remote sensing methods used for estimating water consumed through ET_a. Two of the more recently developed methods are discussed in detail, Mapping Evapotranspiration at High Resolution with Internalized Calibration (METRIC) and Operational Simplified Surface Energy Balance (SSEBop), including the theory behind the continued improvement of these methods and some of their applications in ET_a estimation. Various qualities of these methods, including the extent and spatiotemporal resolution of model estimates and their accuracies, the cost, and the ease of implementation, also are discussed in comparing the usefulness of the two methods for a particular project. This report is not intended to provide a systematic review of all remote sensing methods that have been developed to estimate consumptive water use from ET_a, but rather a synopsis of some recently developed techniques that currently (2017) seem most applicable to ET_a estimation at scales appropriate for water resource management, along with a discussion of the potential for cloud computing to enable the operability of these techniques over large extents at high spatiotemporal resolution.

Review of Remote Sensing Methods for Estimating Actual Evapotranspiration

The use of remote sensing data for estimating ET_a began in the 1970s (Li and others, 2009). Original remote sensing methods have been improved over the years with refinements in modeling the processes that affect ET_a as well as advances in satellite technology and computing power. These developments have meant that fewer ground-based measurements of model parameters are required, and models can be applied more accurately over larger extents at higher spatiotemporal resolution.

Initial Empirical Methods

One of the earliest remote sensing methods for estimating ET_a was a simplified empirical regression model that estimated ET_a from the difference between surface and air temperatures (Jackson and others, 1977):

$$ET_a = R_n - B\left(T_s - T_a\right) \tag{1}$$

where

R_n is net radiation, in watts per square meter;
B is a composite constant related to undefined parameters;
T_s is land surface temperature, in kelvins; and
T_a is air temperature, in kelvins.

Remote sensing data are used to generate R_n and T_s, but T_a is taken from on-the-ground measurements and B requires site-specific parameterization using ordinary least squares fit to empirical data. Jackson and others (1977) determined that this model estimated ET_a reasonably well for a wheat field in Arizona.

Other researchers have revised parameterization of the model of Jackson and others (1977) and have developed modifications (additional exponents and/or coefficients) that improve its scalability and transferability. Seguin and Itier (1983) determined that the model parameters were most strongly influenced by atmospheric stability, wind speed, and surface roughness, which allowed for a more standardized parameterization of the model. Nieuwenhuis and others (1985) tried to ease the constraints of site-specific parameterization using a boundary layer model to simulate the model parameters. Taconet and others (1986) also used a boundary layer model to simulate the model parameters relative to changes in surface roughness, wind speed, and vegetation. Because of these physical factors, ET_a estimates from the Jackson and others (1977) model were determined to be very sensitive to the height above the surface that T_a is measured (Carlson and Buffum, 1989). This finding made it reasonable to use remote sensing data for generating T_a like other parameters in the model. It was shown that T_a became less influenced by surface features when estimated at least 50 meters (m) above the surface, which reduces some of the need for on-the-ground measurements. Moreover, this finding made it possible to scale the model from local to regional extents, although ET_a estimates were produced at a coarse resolution beyond the size of most agricultural plots (Seguin and others, 1994).

The model of Jackson and others (1977) for estimating ET_a is expedient because of its simplicity—the only data requirements being T_s, T_a, and R_n—which has facilitated applications from local to regional scales. This model has been applied successfully in many areas under varied atmospheric conditions and vegetative cover (Nieuwenhuis and others, 1985; Carlson and Buffum, 1989; Seguin and others, 1994); in these three studies, the error in ET_a estimation averaged about 1 millimeter (mm) per day. All these applications, however, are limited by a need for site-specific parameterization that does not allow for transference to new locations. More complex analytical methods have been developed that overcome limitations of this earlier empirical method, and most use some form of the surface energy balance model.

Current Surface Energy Balance Models

More complex remote sensing methods for estimating ET_a are grounded in the theory behind the surface energy balance model (Biggs and others, 2015), also known as the energy balance model, where available energy from shortwave and longwave radiation is balanced by fluxes from the heating of Earth's surface and phase changes of water such as ET_a. The ET_a is estimated by fully or partially solving the energy balance model (Khan and others, 2015):

$$R_n = LE - H - G \tag{2}$$

where

R_n is net radiation, in watts per square meter;
LE is latent heat flux (energy consumed through ET_a), in watts per square meter;
H is sensible heat flux (energy convected to the air), in watts per square meter; and
G is ground heat flux (energy conducted to the ground), in watts per square meter.

Additionally, these methods apply an analytical approach to ET_a estimation using physically based models of varied complexity that require a combination of ground-based and remote sensing data.

Surface energy balance models can be divided into two categories: single-source energy balance models, where vegetation and soil are analyzed in a combined energy budget, and dual-source energy balance models, where vegetation and soil energy budgets are analyzed separately. Single-source energy balance models include Surface Energy Balance Algorithm for Land (SEBAL; Bastiaanssen and others, 1998a), Simplified Surface Energy Balance Index (S-SEBI; Roerink and others, 2000), Surface Energy Balance System (SEBS; Su, 2002), Mapping Evapotranspiration at High Resolution with Internalized Calibration (METRIC; Allen and others, 2007b), and Operational Simplified Surface Energy Balance (SSEBop; Senay and others, 2007; 2013). Dual-source energy balance models include the Two-Source Model (TSM; Norman and others, 1995), Two-Source Time Integrated Model (TSTIM; Anderson and others, 1997), Atmosphere-Land Exchange Inverse (ALEXI; Mecikalski and others, 1999), Dual Temperature Difference (DTD; Norman and others, 2000), and Enhanced Two-Source Evapotranspiration Model for Land (ETEML; Yang and others, 2015).

The premise for using dual-source energy balance models to estimate ET_a is that they better estimate evaporation from bare surfaces, whereas single-source energy balance models are best used for estimating transpiration from vegetated surfaces. However, dual-source energy balance models can require more data and parameterization and do not seem to provide greatly improved estimates of ET_a compared to single-source models (Timmermans and others, 2007; French and others, 2015). The theory and application of many of these methods have already been reviewed in detail (Gowda and others, 2008a; Li and others, 2009; Liou and Kar, 2014) and are beyond the scope of this report. Instead, this report focuses on METRIC and SSEBop, two energy balance models for estimating ET_a that are currently applied successfully in the United States.

Mapping Evapotranspiration at High Resolution with Internalized Calibration (METRIC)

Allen and others (2007a; 2007b) developed METRIC, which is one of the more successfully applied remote sensing methods for estimating ET_a with the energy balance model (eq. 2). The METRIC model can produce maps of ET_a at high spatial resolution (30 m using Landsat data) for specific areas smaller than several hundred square kilometers in extent (Allen and others, 2007a), an improvement in practice over methods used more generally at larger scales. This method has been applied for many purposes, including planning of water resources, modeling of watershed hydrology, mapping of water use by riparian vegetation, monitoring of water rights compliance, evaluation of aquifer depletion from pumpage, and assessment of irrigation performance (Allen and others, 2007a).

Theory

The METRIC model is a further development of the techniques used by SEBAL (Bastiaanssen and others, 1998a). Both models estimate ET_a as a residual of the energy balance at the land surface using equation 2 (Allen and others, 2007b). To compute the parameters in equation 2, METRIC uses shortwave and longwave radiation from satellite imagery, a 30-m digital elevation model (DEM), and hourly ground-based weather data near the study area (Allen and others, 2007b). In brief, METRIC computes net radiation (R_n) from narrowband reflectance and surface temperature; ground heat flux (G) from R_n, surface temperature, and vegetation indices; and sensible heat flux (H) from surface temperature, wind speed, and surface roughness.

Net radiation (R_n) in equation 2 is computed by adding all incoming radiation and subtracting all outgoing radiation:

$$R_n = R_{S\downarrow} - \alpha R_{S\downarrow} + R_{L\downarrow} - R_{L\uparrow} - \left(1-\varepsilon_0\right) R_{L\downarrow} \tag{3}$$

where

$R_{S\downarrow}$ is incoming shortwave radiation, in watts per square meter;

α is surface albedo (dimensionless);

$R_{L\downarrow}$ is incoming longwave radiation, in watts per square meter;

$R_{L\uparrow}$ is outgoing longwave radiation, in watts per square meter; and

ε_0 is broadband surface thermal emissivity (dimensionless).

These intermediate parameters are calculated in METRIC with numerous submodels that apply additional parameters derived from the ground-based weather data, DEM, and satellite imagery (Allen and others, 2007b).

Ground heat flux (G) in equation 2 is computed with one of two alternative submodels (Bastiaanssen, 2000; Tasumi, 2003). Both submodels apply empirical relationships between R_n, α, surface temperature, and a vegetation index to compute G (Allen and others, 2007b). Bastiaanssen (2000) uses normalized difference vegetation index (NDVI) as the vegetation index, whereas Tasumi (2003) uses leaf area index (LAI).

Sensible heat flux (H) in equation 2 is computed with an aerodynamic function:

$$H = \rho_{air} C_p \frac{dT}{r_{ah}} \tag{4}$$

where

ρ_{air} is density of air, in kilograms per cubic meter;

C_p is specific heat of air at constant pressure, in joules per kilogram per kelvin;

dT is temperature difference between two near surface heights, Z_1 and Z_2, in kelvins; and

r_{ah} is aerodynamic resistance (surface roughness and atmospheric stability) between Z_1 and Z_2, in seconds per meter.

Wind speed, elevation, and LAI or NDVI are used to calculate r_{ah} with several submodels in an iterative process (Allen and others, 2007b). The temperature gradient (dT) is calculated with a linear function developed by Bastiaanssen (1995):

$$dT = a + bT_{s\ datum} \tag{5}$$

where

a is the intercept;

b is the slope; and

$T_{s\ datum}$ is land surface temperature adjusted to a standard elevation per pixel of the satellite image, in kelvins.

The parameter $T_{s\ datum}$ corrects for temperature change within a satellite image that is related to elevational change but unrelated to dT or H (Allen and others, 2007b).

The METRIC model reduces the complications of other methods that use the surface energy balance model (eq. 2) by focusing its calibration on computing H and internalizing the errors and biases associated with computing LE (Allen and others, 2007b). This calibration primarily depends on dT, which is indexed to surface temperature estimated radiometrically rather than measured on the ground, simplifying the computation of H. Two reference pixels are used to define the evaporative extremes of the energy balance at the land surface. Both pixels are chosen by the user to represent the range of dT over the land surface. A “cold” (also called “wet”) reference pixel is selected in a well-irrigated field with full vegetative cover where ET_a is assumed to equal reference evapotranspiration (ET_r). The standardized Penman-Monteith equation (American Society of Civil Engineers, 2005) is used to calculate ET_r. The sensible heat flux for the cold pixel (H_{cold}) is calculated with the energy balance model:

$$H_{cold} = \left(R_n - G\right)_{cold} - LE_{cold} \tag{6}$$

where

$R_{n\ cold}$ is net radiation at the cold pixel, in watts per square meter;

G_{cold} is ground heat flux at the cold pixel, in watts per square meter; and

LE_{cold} is latent heat flux at the cold pixel, in watts per square meter.

Research has shown that the coldest (wettest) agricultural fields have ET_a rates about 5 percent greater than those for a reference alfalfa crop (Tasumi and others, 2005a), so for the cold pixel, the ratio of LE to ET_r is assumed to be 1.05; however, this assumption does not apply outside of, or at the beginning of, the growing season when the abundance of vegetation is much less than that of the reference alfalfa crop. During these times of the growing season, a more appropriate ratio of LE to ET_r for the cold pixel can be calculated with a function of NDVI defined by the user (Allen and others, 2007b). The temperature gradient for the cold pixel (dT_{cold}) is calculated with the inverse of equation 4:

$$dT_{cold} = \frac{H_{cold} r_{ah\ cold}}{\rho_{air\ cold} C_p} \qquad (7)$$

where

H_{cold} is sensible heat flux at the cold pixel, in watts per square meter;

$r_{ah\ cold}$ is surface roughness and atmospheric stability at the cold pixel, in seconds per meter;

$\rho_{air\ cold}$ is density of air at the cold pixel, in kilograms per cubic meter; and

C_p is specific heat of air at constant pressure, in joules per kilogram per kelvin.

The "hot" (also called "dry") reference pixel is chosen in a dry, bare field where ET_a is assumed to be zero. Unlike SEBAL, METRIC verifies this assumption with a daily soil water balance model, which determines whether evaporation is greater than zero because of antecedent moisture (Allen and others, 2007b). The calculations of H and dT for the hot pixel are the same as those for the cold pixel (eqs. 6 and 7, respectively). The values for dT and $T_{s\ datum}$ for the hot and cold pixels are used to calculate the two coefficients (a, b) in equation 5:

$$a = \frac{dT_{hot} - dT_{cold}}{T_{s\ datum\ hot} - T_{s\ datum\ cold}} \qquad (8)$$

$$b = \frac{dT_{hot} - a}{T_{s\ datum\ hot}} \qquad (9)$$

where

$dT_{hot/cold}$ is temperature gradient at the hot/cold pixel, in kelvins; and

$T_{s\ datum\ hot/cold}$ is land surface temperature at the hot/cold pixel adjusted to a standard elevation per pixel of the satellite image, in kelvins.

Once the user determines the linear relationship between dT and $T_{s\ datum}$ (eq. 5), H is computed for each pixel of the satellite image.

The values for G and H are subtracted from that of R_n to compute LE, the energy consumed through ET_a. Subsequently, LE is used to estimate ET_a for each pixel of the satellite image:

$$ET_{inst} = 3600 \frac{LE}{\lambda \rho_w} \qquad (10)$$

where

ET_{inst} is instantaneous ET_a (depth of liquid evaporated at the time of the satellite image), in millimeters per hour;

3600 is a factor for converting from seconds to hours;

LE is latent heat flux, in watts per square meter;

λ is latent heat of vaporization, in joules per kilogram; and

ρ_w is density of water (about 1,000 kilograms per cubic meter).

The ET_a is extrapolated to a daily time scale by calculating ET_r fraction (ET_rF), which is equivalent to the crop coefficient for the cold pixel (Allen and others, 2007b):

$$ET_rF = \frac{ET_{inst}}{ET_r} \qquad (11)$$

where

ET_{inst} is instantaneous ET_a, in millimeters per hour; and

ET_r is reference ET at the time of the satellite image, in millimeters per hour.

It is assumed that ET_rF is constant throughout the day—an assumption that Allen and others (2007b) verified with observational data—and ET_rF is used to calculate daily ET_a (ET_{24}):

$$ET_{24} = ET_rF \times ET_{r24} \qquad (12)$$

where

ET_rF is ET_r fraction (dimensionless); and

ET_{r24} is ET_r cumulated over 24 hours on the date of the satellite image, in millimeters.

With the assumption that ET_a for the study area varies in proportion to changes in ET_r at the weather station, ET_a is extrapolated to a monthly or seasonal period (ET_{period}) by interpolating ET_rF between successive dates of satellite images (using a linear or curvilinear function) and multiplying by ET_r for each day:

$$ET_{period} = \sum\nolimits_{i=m}^{n} \left(ET_rF_i \times ET_{r24i} \right) \qquad (13)$$

where

ET_{period} is ET_a cumulated over a period from days *m* to *n*, in millimeters;

ET_rF_i is ET_rF interpolated over day *i* (dimensionless); and

ET_{r24i} is ET_r cumulated over 24 hours for day *i*, in millimeters.

One satellite image for each month can be sufficient to estimate seasonal ET_a (Allen and others, 2007b), but during times of rapid vegetative growth, multiple dates of satellite images may be needed. In addition, one weather station can be adequate for calculating ET_r (Allen and others, 2007b), but if the study area is very heterogeneous and multiple stations are available, the user may need to apply METRIC to separate sections in the study area.

Lastly, unlike SEBAL, METRIC uses ET_rF to extrapolate ET_a from instantaneous to daily instead of using the evaporative fraction (*EF*), which is the ratio of ET_a to available energy ($R_n - G$). Research has shown that *EF* underestimates daily ET_a in drier climates (Allen and others, 2007b), whereas ET_rF incorporates changing weather such as wind and humidity that affect advection of heat throughout the day because these changes are integrated in the calculation of ET_r, which is done hourly and summed over 24 hours.

Application

Several studies have compared on-the-ground measurements of ET_a to satellite-based estimates from METRIC. Estimates of ET_a from METRIC were compared to measurements from lysimeters near Montpelier, Idaho, for a 150- by 300-kilometer (km) portion (two Landsat scenes) of the Bear River basin (Allen and others, 2007a). Measurements of ET_a were taken with lysimeters located near an irrigated field of a native sedge forage crop that was characteristic of the area. Estimates of ET_a were made with METRIC for a field close to the lysimeters on four dates throughout the 1985 growing season. The least accurate monthly ET_a estimate was for July 14, which had a difference of 28 percent between the estimated and measured ET_a; however, this difference was deemed reasonable because of vegetation growing rapidly at that time and precipitation preceding the date of the satellite image. The average difference between monthly ET_a estimated with METRIC and that measured with the lysimeters was plus or minus 16 percent. When data for the growing season were compared, the difference was only 4 percent, which was attributed to the reduction in random errors associated with each monthly METRIC estimate and lysimeter measurement (Allen and others, 2007a).

Estimates of ET_a from METRIC also were compared to lysimeter measurements on the Snake River Plain near Kimberly, Idaho, on eight dates of Landsat 5 scenes during the 1989 growing season (Allen and others, 2007a). The lysimeters had been measuring ET_a for more than 20 years over a range of ground cover and weather conditions, enabling comparisons of those measurements to estimates of ET_a from METRIC over various times of the growing season and for various crop types and growth stages. This study showed that METRIC functioned consistently across clear, partly cloudy, and cloudy days, validating the assumption that ET_rF for a daily time scale can be estimated by instantaneous ET_rF at the time of the satellite image. Estimates of ET_rF for the 24-hour period were within 5 percent of instantaneous ET_rF in nearly all samples for clipped grass and sugar beets. Estimates of ET_a from METRIC were least accurate during the early and late growing season, which had differences of 139 percent for April 18 and 34 percent for September 25, although the difference for April 18 was partially attributed to drying of recently wetted bare ground. When omitting the value for April 18, the average difference was 14 percent. Like the study from Montpelier, Idaho, this difference decreased when data for the growing season were compared. Measured by the lysimeters, the seasonal ET_a of the sugar beet crop was 718 mm, whereas the estimate from METRIC was 714 mm, a difference of less than 1 percent (Allen and others, 2007a).

Estimates of ET_a from METRIC also have been compared to those made with SEBAL. The two models were applied independently in southern Idaho to two partially overlapping Landsat 5 and 7 scenes in 2000 (Tasumi and others, 2005b). These independent applications of METRIC and SEBAL involved different users, different pathways and dates for the Landsat scenes, different weather stations, and different choices of the hot and cold reference pixels. Monthly and seasonal estimates of ET_a made with SEBAL and METRIC were compared for pixels sampled from the overlapping portion of the Landsat scenes. The seasonal estimates of ET_rF from METRIC and *EF* from SEBAL were consistent and repeatable; coefficients of determination (r^2; Helsel and Hirsch, 2002) were 0.59 and 0.58 and standard deviations were 0.06 percent and 0.05 percent, respectively, in comparisons of the two scenes. The monthly estimates had more variability because data were less available in some months. These applications demonstrated the value of METRIC for estimating ET_a of agriculture in the semi-arid western United States.

Another application of METRIC has been to improve estimates of water balance models that have used empirical models, rather than a physically based surface energy balance model, to estimate ET_a. Using METRIC to estimate ET_a, Santos and others (2008) applied a water balance model to produce more efficient irrigation schedules for the Genil-Cabra Irrigation Scheme of Spain. The high temporal resolution of the water balance model and the high spatial resolution of the satellite imagery provided near real-time estimates of ET_a from METRIC to improve irrigation scheduling for individual agricultural plots. The study area consisted of 6,800 hectares (ha) of irrigated farmland with a diversity of crop types, including wheat, cotton, olive, maize, sugar beet, beans, garlic, sunflower, and other vegetables. Landsat scenes on 11 dates in 2004–5 and weather data from five ground-based stations were used to make estimates with the model. Among plots, estimates of ET_a from METRIC ranged from 0 mm for non-agricultural fields in the study area to 1,000 mm for some well-irrigated plots of sugar beet. The estimates showed high variability in crop coefficients (ET_a from METRIC divided by ET_r) among the crop types, suggesting in part suboptimal irrigation scheduling. In addition, the estimates showed great variability within plots, ranging from 70 mm for pepper (12 percent of seasonal ET_a) to 160 mm for sunflower (44 percent of seasonal ET_a). Using the model estimates to update the irrigation schedule in real-time would have reduced the watering depth from 733 mm to 559 mm for cotton, a 24-percent decrease in water use, but would have increased water use for sugar beet by 21 percent. Estimated ET_a from METRIC for selected crops and plots was 677 mm, whereas the measured delivery of irrigation water was 699 mm, an error of 3 percent. In this application, METRIC provided estimates of ET_a at high spatiotemporal resolution, improving irrigation performance and water consumption throughout the growing season for individual agricultural plots.

Gowda and others (2008b) applied METRIC to ET_a estimation in the Texas High Plains near Lake Meredith in agricultural fields dependent on irrigation water pumped from the Ogallala Aquifer. The study area encompassed 234,000 ha, about one-half of which were planted with corn, cotton, sorghum, soybean, and wheat, and the rest had interspersed semi-arid shrubs and grasses. The study area experiences strong winds and temperature gradients across the landscape during the growing season, affecting advection of heat, which is responsible for more than half of ET_a. Estimates of ET_a were made with METRIC using Landsat 5 scenes on two dates (June 27 and July 29) in 2005 and ground-based weather data from four stations. Estimates of ET_a in four fully or partially irrigated fields of corn and cotton, experiencing varied water stress, were compared to a daily soil water balance model. The partially irrigated cotton field had relatively high differences between estimated and measured ET_a, potentially because of less plant biomass and more bare soil. When omitting the values for this field, the average difference was 13 percent and -5 percent on June 27 and July 29, respectively, which Gowda and others (2008b) deemed exceptional given the prevailing weather conditions that promote advection of heat.

Most applications of METRIC have been at local scales at high spatial (30 m) but lower temporal (8–16 days) resolution using data from Landsat 5, 7, and 8. Few studies have attempted to apply METRIC or SEBAL at regional scales at lower spatial (250–1,000 m) but higher temporal (1–2 days) resolution using data from Moderate Resolution Imaging Spectroradiometer (MODIS). Data from MODIS were used in applications of SEBAL in Brazil and China (Ruhoff and others, 2012; Yang and others, 2012). Trezza and others (2013) used METRIC with MODIS data in a study of a 3- by 3-degree section of the Middle Rio Grande Basin in New Mexico. The main difficulty in using METRIC with low spatial resolution (1 km) MODIS data is the selection of hot and cold reference pixels that are uniform within 1 square kilometer (km^2), the area of a pixel. To overcome this limitation, the cold pixel was chosen with a procedure that incorporated MODIS and Landsat 5 data, whereas the hot pixel selection was made with MODIS data. Comparisons were made between METRIC estimates of ET_a using MODIS and Landsat 5 data for scenes on 13 dates in 2002. Estimates of ET_a using data from MODIS were lower than those made with Landsat for pixels with high NDVI but comparable for pixels with low NDVI. Moreover, ET_a estimates made with MODIS data were highly correlated with those using Landsat ($r^2 = 0.9$); annual ET_a averaged over the Middle Rio Grande Basin was 1,045 mm with MODIS and 1,067 mm with Landsat. Uncertainty of ET_a estimates for individual agricultural plots, however, was very high when using METRIC with MODIS data.

Operational Simplified Surface Energy Balance (SSEBop)

Senay and others (2013) developed SSEBop, which is the most recent revision of Simplified Surface Energy Balance (SSEB; Senay and others, 2007). Because SSEBop builds on the theory from SSEB, this section will focus first on SSEB and then discuss its progression toward SSEBop. Similar to METRIC, SSEBop is another remote sensing method that applies the simplified version of the surface energy balance model (eq. 2) to estimate ET_a. Applications of this method also have had many purposes, including drought monitoring and famine early warning in regions with sparse ground-based data, mapping of water use by different land cover classes, and estimation of ET_a in the United States at regional to continental scales (Senay and others, 2007; 2011a; 2013; 2016). The SSEBop model has been used to produce maps of ET_a over very large extents (the conterminous United States) using lower spatial resolution (1 km) MODIS data (Senay and others, 2016). Unlike METRIC, SSEBop requires less parameterization of the energy balance model, making for simpler application over larger extents, and does not have the same requirements for finely resolved ground-based data such as hourly weather information.

Theory

The SSEB model functions similarly to METRIC (Allen and others, 2007b). The METRIC model assumes that variation in land surface temperature (LST) is linearly related to the temperature difference between the land surface and air. This relation is defined through the selection of two reference pixels: a hot pixel that represents bare, dry fields; and a cold pixel that represents vegetated, wet fields. The temperature gradient is used in equation 2 to estimate H (sensible heat flux), which is assumed to vary linearly between the hot and cold pixels. This assumption holds for SSEB, where it is further assumed that LE in equation 2 (energy consumed through ET_a) also varies linearly between the hot and cold pixels. Senay and others (2007) remark that this assumption is supported by research showing that the temperature difference between the land surface and air is linearly related to soil moisture. They additionally assume that ET_a can be inferred from the temperature gradient, which can be estimated from land surface temperatures of the hot and cold pixels. At the hot pixel, ET_a is assumed to be zero, and ET_a at the cold pixel is assumed to be maximal—that is, to equal ET_r. At all other pixels in a study area, ET_a is scaled proportionately to the surface temperature of each pixel in relation to that of the hot and cold pixels. With this assumption, fractional evapotranspiration (ET_f) is calculated for each pixel:

$$ET_f = \frac{T_h - T_s}{T_h - T_c} \tag{14}$$

where

T_h is LST for the hot pixel, in kelvins;
T_s is LST of each pixel, in kelvins; and
T_c is LST for the cold pixel, in kelvins.

To calculate the parameters in equation 14, SSEB uses satellite imagery for LST and a vegetation index (NDVI) to assist in choosing the hot and cold reference pixels. From the study area, regions of high temperature and low NDVI (hot, bare fields) and low temperature and high NDVI (cold, well-vegetated fields) are identified from which the hot and cold reference pixels are chosen. The ET_a is calculated from ET_f for each pixel in the study area:

$$ET_a = ET_f \times ET_0 \tag{15}$$

where

ET_f is fractional ET (dimensionless); and
ET_0 is reference ET, in millimeters.

Available gridded data such as those from the Global Data Assimilation System (GDAS) model are used to calculate ET_0, which results in a 1-degree grid of global daily data (Senay and others, 2008). The GDAS model uses the standardized Penman-Monteith equation (American Society of Civil Engineers, 2005) to compute ET_0 for a shortgrass crop (Allen and others, 1998). Senay and others (2007) disaggregate the 1-degree data from this model onto a 10-km grid. However, if ET_0 is available from a weather station, ET_a estimates will likely be more accurate using the local values of ET_0.

A major assumption of SSEB is that differences in LST over a homogeneous landscape are related to differences in vegetation and its water use (Senay and others, 2007). Because this assumption ignores α and G, ET_a is underestimated for surfaces with low albedo (light reflectance) and overestimated for surfaces with high albedo and high ground heat flux, such as bare soils (Senay and others, 2011a). In addition, SSEB assumes that LST and ET_a are linearly related, but this assumption is questionable if α and G of a pixel on the landscape differ greatly from that of the reference crop (Senay and others, 2011a). To better support these assumptions, Senay and others (2011a) developed an adaptation of SSEB (SSEBelvi) with a correction for elevation with a DEM and another correction for land cover with a vegetation index. These modifications were developed to improve SSEB in applications on landscapes with varied elevation, slope, or aspect, and with mixed bare soil and green or senesced vegetation.

To improve SSEB for applications not just on flat, irrigated fields but also on more complicated terrain, LST is corrected for topographic differences:

$$LST_c = LST + K_L \times DEM \tag{16}$$

where

LST_c is LST corrected for elevation, in kelvins;
LST is uncorrected LST, in kelvins;
K_L is lapse rate in temperature of air moving over the landscape, in kelvins per meter; and
DEM is land surface elevation from a digital elevation model, in meters.

The standard value for the lapse rate is 0.0065 kelvins per meter. When using SSEBelvi, LST_c is substituted for LST to calculate ET_f in equation 14.

To improve the application of SSEB for mixed land cover, NDVI is used to correct for vegetation differences:

$$ET_{f(elvi)} = \left(0.35 \times \frac{NDVI}{0.7} + 0.65\right) \times ET_{f(el)} \tag{17}$$

where

$ET_{f(elvi)}$ is ET_f corrected for elevation and vegetation index (dimensionless);
$NDVI$ is normalized difference vegetation index (dimensionless); and
$ET_{f(el)}$ is ET_f from equation 14 corrected for land surface elevation (dimensionless).

With SSEBelvi, it is assumed that if the NDVI value of a pixel is greater than 0.7, that pixel is well-vegetated and will have ET_a greater than that of the reference crop if water is not limiting (Senay and others, 2011a). The possible range of the coefficient in equation 17 (the resulting value of all terms within the parentheses) is 0.65–1.15, but the probable maximum is 1.05 because NDVI is rarely greater than 0.8 for a pixel. Senay and others (2011a) state that this range has no strong theoretical basis, but that the probable maximum is equivalent to the correction factor used by METRIC (1.05) for calculating ET_f of the cold reference pixel. When using SSEBelvi, $ET_{f(elvi)}$ is substituted for ET_f to calculate ET_a in equation 15.

To reduce the potential for bias from the user selecting the hot and cold reference pixels in SSEB and SSEBelvi, SSEBop was developed with a procedure similar to that of SEBS (Su, 2002) to predetermine the difference between the hot and cold boundary conditions for each pixel (Senay and others, 2013). The SSEBop model, unlike METRIC, SSEB, and SSEBelvi, does not require the user to select the hot and cold reference pixels for a study area. The only data required are T_s, T_a, and ET_0. Senay and others (2013) state that their model is boldly simple, but that it is grounded in knowledge that available R_n drives the surface energy balance model. They argue that under clear skies the hot and cold boundary conditions do not vary significantly among years, and more importantly the difference between the hot and cold reference values can be assumed constant for a given location and day of year. With this assumption, ET_a is calculated as a fraction of ET_0:

$$ET_a = ET_f \times kET_0 \tag{18}$$

where

ET_f is fractional ET (dimensionless);

k is a coefficient that scales ET_0 to maximum ET_a of a less aerodynamic crop; and

ET_0 is reference ET for a shortgrass crop, in millimeters.

The standard value for the coefficient is 1.2, but it also can be determined with calibration procedures using soil water balance or surface energy balance approaches, or field data (Senay and others, 2013). The idealized hot and cold reference values for each pixel are used to calculate ET_f in equation 14.

It is assumed that under clear-sky conditions ET_a will be equivalent to potential ET if T_s is similar to T_a (H is minimal), so daily maximum air temperature (T_a) can be multiplied by a correction factor to calculate land surface temperature for the cold pixel (T_c) in equation 14:

$$T_c = cT_a \tag{19}$$

where

c is a coefficient that relates T_s to T_a for well-irrigated vegetation at maximum ET_a; and

T_a is air temperature, in kelvins.

This assumption can be verified by relating T_s to T_a from remote sensing data for well-irrigated vegetation in the study area.

Land surface temperature for the hot pixel (T_h) is calculated by adding the temperature difference to T_c from equation 19:

$$T_h = T_c + dT \tag{20}$$

where

T_c is land surface temperature for the cold pixel, in kelvins; and

dT is temperature gradient between the idealized hot and cold reference values for each pixel, in kelvins.

The parameter dT is predetermined for each pixel and day of year by partially solving the energy balance model for dry, bare soil where it is assumed that ET_a is zero and H is maximal (Bastiaanssen and others, 1998a; Allen and others, 2007b). Because LE and G in equation 2 are assumed to be zero at a daily time scale for bare, dry soil, R_n can be estimated as H in equation 4, and dT can be calculated with the inverse of equation 4. Senay and others (2013) used a trial-and-error calibration approach to determine r_{ah}, which they fix at 110 seconds per meter, a value also found in the range reported by other research (Qiu and others, 1998).

Lastly, satellite imagery can underestimate T_s on some non-vegetated surfaces with high albedo, such as desert sands, or high emissivity, such as lava rocks. Consequently, SSEBop may overestimate ET_a for these surfaces. To correct for this misinterpretation of T_s when using SSEBop to estimate ET_a, either a mask is applied over these surfaces or a correction factor is used with α to increase T_s.

Application

The SSEB, SSEBelvi, and SSEBop models have been applied at local, regional, and continental scales, and tested against more complex remote sensing methods for estimating ET_a. Senay and others (2007) used SSEB to estimate ET_a in irrigated agricultural lands in two river basins in Afghanistan during 2000–5. Because these river basins had varied temperature gradients, they were each divided by elevation into three subdivisions, ranging in size from 430 to 2,100 km^2. Irrigated fields were delineated with data from Landsat, MODIS, and Advanced Spaceborne Thermal Emission and Reflection Radiometer (ASTER). Afghanistan lacked field data for model validation, but spatial and temporal patterns of estimated ET_a were consistent with observations of vegetative cover from NDVI, estimates of ET_a from a water balance model, and published reports of precipitation (Senay and others, 2007). Furthermore, in a preliminary validation of SSEB against METRIC applied to corn and soybean fields in South Dakota in 2001 with Landsat data (Senay and others, 2007), ET_a estimates from both models were highly correlated (r^2 greater than 0.9).

Satellite-based estimates of ET_a from SSEB have been compared to on-the-ground measurements in several studies. Estimates of ET_a using SSEB were compared to measurements taken with lysimeters near Bushland, Texas, on the Southern High Plains (Gowda and others, 2009). Lysimeters measured ET_a in dryland and irrigated agricultural plots planted with corn and sorghum. Estimates of ET_a were made with SSEB for Landsat scenes on 14 dates during the 2007 and 2008 growing seasons. Estimates of ET_a from SSEB explained 84 percent of the variance in the daily measurements from lysimeters, and had a root mean square error (RMSE; Helsel and Hirsch, 2002) of 1.2 mm. The differences between SSEB and the lysimeters mostly involved the dryland agricultural plots; SSEB overestimated ET_a at lower values (less than 2.5 mm) of lysimeter-measured daily ET_a and underestimated ET_a at higher values. It was determined that SSEB performed comparably to more complex energy balance models at estimating ET_a in semi-arid landscapes. Gowda and others (2009) concluded that SSEB is promising for regional-scale applications because of its simplified approach with minimal data requirements.

Estimates of ET_a made with SSEB also have been compared to those from a water balance model (Senay and others, 2011b). For 1,399 eight-digit hydrologic unit code (HUC8) subbasins in the conterminous United States, ET_a

was estimated using SSEB and was modeled as the difference between precipitation and runoff (Senay and others, 2011b). The comparison was made with the median values for precipitation and runoff for 2000–9. Estimates of ET_a from SSEB and the water balance model were highly correlated (r^2 greater than 0.9) and had a mean error of -67 mm (11 percent of the difference between precipitation and runoff). Senay and others (2011b) ascertained that SSEB showed the expected patterns of ET_a across the contiguous United States but underestimated ET_a in more arid regions. This underestimation most likely was due to the low spatial resolution (1 km) of MODIS data, which assimilates land within a 1-km^2 pixel that may not be contributing to ET_a.

Senay and others (2011a) compared spatial and temporal variation in ET_a estimates from SSEBelvi to those from METRIC for agricultural fields in southern Idaho. Spatial variation in ET_a estimates was compared for the whole study area on June 28, 2003, and temporal variation in ET_a estimates was compared for six plots in Landsat scenes on seven dates throughout the 2003 growing season. For pixels in the study area at elevations less than 2,000 m, where the terrain was homogeneous, spatial variation in ET_a estimates from SSEBelvi and METRIC were highly correlated, having a correlation coefficient (*r;* Helsel and Hirsch, 2002) of 0.95. For pixels greater than 2,000 m in elevation, which had more complicated terrain, SSEBelvi tended to overestimate ET_a at lower values of ET_a estimated with METRIC; however, the corrections for elevation and vegetative cover with a DEM and NDVI were determined to improve the correlation between SSEB and METRIC for pixels at higher elevations ($r = 0.62$). Temporal variation in ET_a estimates also was comparable between SSEBelvi and METRIC for most of the agricultural plots. Although SSEBelvi tended to overestimate ET_a earlier in the growing season, it was similar to METRIC later in the growing season when daily or monthly ET_a is much greater. Senay and others (2011a) surmised that selecting the cold reference pixel in a water body would help reduce this error.

Two studies have compared SSEBop estimates of ET_a to eddy covariance measurements (Senay and others, 2013; Chen and others, 2016). In both studies, ET_a estimates were compared to measurements taken at more than 40 flux towers covering diverse ecosystems across the contiguous United States, including cropland, grassland, forest, shrubland, and woody savanna. Senay and others (2013) parameterized SSEBop with monthly air temperature data in 2005 from Parameter-Elevation Regressions on Independent Slopes Model (PRISM) and found high correlation between monthly ET_a estimates from SSEBop and eddy covariance measurements ($r^2 = 0.64$; RMSE = 27 mm). Senay and others (2013) concluded that SSEBop is promising for applications at a continental scale given the minimal data requirements and the consistency of model estimates produced by different users. Chen and others (2016) parameterized SSEBop for monthly data during 2001–7 and determined that across five land cover classes, SSEBop estimates of ET_a explained 86 percent of the variance in the monthly eddy covariance measurements and had an RMSE of 15 mm. The model performed best for cropland ($r^2 = 0.92$; RMSE = 13 mm). A sensitivity analysis of the model determined that errors in all six parameters might cause errors in ET_a estimation as great as 30 percent, and that the model is most sensitive during the non-growing season and in more arid regions. Despite the potential for error in parameterizing SSEBop, Chen and others (2016) determined that uncertainty in the simplification of the model did not significantly affect how well SSEBop estimates ET_a at a regional scale.

Singh and Senay (2016) compared ET_a estimates from SSEBop to those from three different energy balance models (METRIC, SEBAL, and SEBS) for irrigated and non-irrigated farmlands in the midwestern United States. Estimates of ET_a were made with Landsat scenes on seven dates throughout the 2001 growing season over three sites planted with maize and soybean. Estimates of ET_a from METRIC, SEBAL, SEBS, and SSEBop were compared to eddy covariance measurements taken at the three sites. Singh and Senay (2016) determined that all four models demonstrated similar spatial and temporal patterns of ET_a. Performance of the models was evaluated with four metrics: r, r^2, Nash-Sutcliffe efficiency (NSE), and RMSE. The NSE compares the relative fit of model simulations to observed data and ranges from negative infinity to 1, with 1 being the optimal value and values less than 0 being worse than the mean observed value (Nash and Sutcliffe, 1970). When compared to eddy covariance measurements, estimates of ET_a made with METRIC had an r, r^2, NSE, and RMSE of 0.96, 0.92, 0.87, and 93 mm, respectively; for SSEBop, they were 0.96, 0.92, 0.90, and 84 mm, respectively.

Two studies have used ET_a estimated with SSEBop to help improve water resource management in the Colorado River Basin (Singh and others, 2014a; Senay and others, 2016). In both studies, ET_a was estimated with Landsat and MODIS data for 144 HUC8 subbasins. Singh and others (2014a) determined there was high correlation between SSEBop estimates of annual ET_a made with high spatial resolution (30 m) Landsat data and eddy covariance measurements taken at seven sites in 2000 ($r^2 = 0.78$); removing two sites affected by wildfire further increased the correlation ($r^2 = 0.95$). Moreover, annual ET_a estimates from SSEBop for the HUC8 subbasins were highly correlated with those from a water balance model ($r^2 = 0.85$). Singh and others (2014b) also determined that estimates of annual ET_a made with SSEBop using lower spatial resolution (1 km) MODIS data had high correlation to those made with Landsat data ($r^2 = 0.79$). However, ET_a estimates made with MODIS data were not spatially explicit enough to manage water resources at the field scale. Senay and others (2016) determined that SSEBop estimates of daily ET_a were highly correlated to eddy covariance measurements taken at two sites (r^2 greater than or equal to 0.82; RMSE less than or equal to 0.6 mm), and annual ET_a estimated with SSEBop had high correlation to that from a water balance model ($r^2 = 0.78$; RMSE = 77 mm). To increase the temporal resolution of ET_a estimates, SSEBop was parameterized with daily air temperature data from Daymet (Thornton and others, 1997). Senay and others (2016) analyzed ET_a by 16 land cover classes and determined that shrubland, the dominant land cover, consumed 146 cubic kilometers (km^3) of water, whereas cropland consumed 4 km^3. However, they determined that precipitation only provided 26–43 percent of water used by cropland in five irrigation districts, emphasizing the value of the high spatiotemporal resolution estimates to managing water resources.

Comparison of METRIC and SSEBop Models

The METRIC and SSEBop models each have been shown to estimate ET_a with acceptable accuracies in many applications. A robust remote sensing method for estimating ET_a, METRIC has been applied successfully in the United States and internationally, and METRIC and SEBAL (the model from which METRIC was developed) have been used to estimate ET_a in more than 25 countries and on all continents except Antarctica (Bastiaanssen and others, 1998b; 2005; Allen and others, 2007a). The SSEBop model largely has been used to estimate ET_a in the United States (Senay and others, 2007; 2011a; 2013; 2016). The METRIC and SSEBop models have many similarities (table 1), including their theoretical grounding in the surface energy balance model and their ability to incorporate low (1 km) and high (30 m) spatial resolution data from MODIS and Landsat; however, they have important differences in data requirements, ease of implementation, and cost.

The METRIC model has shown greater accuracy at estimating ET_a than simpler techniques that use crop coefficients or vegetation indices exclusively (Choudhury and others, 1994; Allen and others, 1998), and also removes the need to know crop type and growth stage (Allen and others, 2011a). The model can detect reductions in ET_a from water shortages, soil salinity, and frozen soil, and can detect evaporative losses from bare soil. In addition, many studies validating METRIC estimates of ET_a against measurements from lysimeters have shown model accuracies on daily to seasonal time scales ranging from 85 to 95 percent (Allen and others, 2007a).

The METRIC model is accurate and accounts for all terms of the energy balance model (table 1). The greater complexity of METRIC results in greater data requirements, including remote sensing data in the visible, near-infrared, and infrared regions of the electromagnetic spectrum, as well as on-the-ground measurements of wind speed and air temperature. Some of the complexity of solving the energy balance model is mitigated by the internalized calibration of METRIC, which reduces data requirements compared to more complex energy balance models; however, this internalized calibration leads to greater skill required for implementation compared to SSEBop.

Skill is required in the selection of the hot and cold reference pixels by the user, which is the principal determinant of the accuracy of METRIC. Long and Singh (2013) demonstrated that context dependency can affect this selection by the user. An appropriate reference pixel may not exist within a satellite image if all the land cover is vegetated (or non-vegetated), or the choice of the reference pixels can be affected if the extent or resolution of the satellite image changes, which in turn would change estimates of ET_a. User error in choosing the hot and cold reference pixels is the greatest source of error in ET_a estimates from METRIC. To apply METRIC appropriately, the user needs background in the theoretical basis of the surface energy balance model and knowledge of the biophysics of vegetation. This user training and the sophistication of the physically based model means that METRIC can cost more than $75,000 per year (in 2004 dollars) to estimate ET_a for a Landsat scene (Allen and others, 2005b). Although METRIC may cost less than estimating ET_a for a study area using crop coefficient techniques with on-the-ground measurements of reference ET, it is still expensive for a 1-year application.

Because of the training needed to apply METRIC properly and the variability in ET_a estimates among even trained users, effort has been made to automate the calibration of METRIC (Allen and others, 2013). Morton and others (2013) developed an algorithm that might simplify ET_a estimation with METRIC. Six trained users manually calibrated METRIC for estimating ET_a with Landsat scenes from 2006 for a study area in Nevada. Statistics from empirical cumulative distribution functions of the selection of the hot and cold reference pixels by these users were used to parameterize the automated calibration algorithm. Comparisons of daily ET_a estimates from the automated calibration to Bowen ratio and eddy covariance measurements at eight sites showed high correlation ($r^2 = 0.8$). Morton and others (2013) affirmed that the automated calibration algorithm compared well to manual selection of the reference pixels, but that more validation is needed in other study areas with different crop types and growing conditions. The automated algorithm for selecting reference pixels is a promising development toward greater objectivity in METRIC estimates of ET_a, and more importantly a more user-friendly means of implementation.

In contrast, SSEBop is a simpler model (table 1), having reduced data requirements and greater ease of implementation without a substantial loss of accuracy in estimating ET_a. Performance has improved greatly from SSEB to SSEBelvi and SSEBop. Like other energy balance models, SSEBop does not perform as well on more complicated terrain, but Senay and others (2013) have suggested further adaptations of the model that may include corrections for slope and aspect in calculating net radiation. Additionally, model accuracies ranging from 80 to 95 percent on daily to annual time scales have been shown in numerous studies that validated ET_a estimates from SSEBop against eddy covariance measurements (Senay and others, 2013; Chen and others, 2016).

The data requirements of SSEBop are air temperature, albedo, land surface elevation, NDVI, net radiation, reference ET, and land surface temperature, most of which are taken from remote sensing data (table 1). Although greater

Table 1. Comparison of the Mapping Evapotranspiration at High Resolution with Internalized Calibration (METRIC) and Operational Simplified Surface Energy Balance (SSEBop) models.

[MODIS, Moderate Resolution Imaging Spectroradiometer; DEM, digital elevation model; ET, evapotranspiration; NDVI, normalized difference vegetation index; LAI, leaf area index; PRISM, Parameter-Elevation Regressions on Independent Slopes Model; GDAS, Global Data Assimilation System; dT, temperature difference between two near-surface heights (temperature gradient)]

Models	Parameters[1]	Sources	Assumptions	Advantages	Disadvantages	References
METRIC	Air temperature Albedo Land surface elevation Ground heat flux Net radiation NDVI or LAI Reference ET Sensible heat flux Land surface temperature Wind speed	Weather stations MODIS or Landsat DEM Internally modeled Internally modeled MODIS or Landsat Weather stations Internally modeled MODIS or Landsat Weather stations	1) Variation in land surface temperature is linearly related to difference between land surface and air temperatures; 2) Sensible heat flux varies linearly between hot and cold reference pixels; 3) Actual ET for hot reference pixel is 0; 4) Ratio of actual ET for cold reference pixel to reference ET is 1.05; 5) Reference ET fraction is constant throughout day; 6) Actual ET for study area varies in proportion to changes in reference ET at weather stations.	1) Minimum ground-based measurements required; 2) Solves for all terms of energy balance model; 3) Land surface slope and aspect can be applied on more complicated terrain.	1) Uncertainty from user selection of hot and cold reference pixels; 2) Costly (as much as $75,000 [in 2004 dollars] per Landsat scene; model use is proprietary to the University of Idaho); 3) Time intensive to apply at basin scale.[2]	Allen and others, 2005b, 2007a, 2007b, 2011a, 2013; Tasumi and others, 2005b; Trezza and others, 2013.
SSEBop	Air temperature Albedo Land surface elevation NDVI Net radiation Reference ET Land surface temperature	PRISM or Daymet MODIS or Landsat DEM MODIS or Landsat Internally modeled GDAS MODIS or Landsat	1) Variation in land surface temperature is linearly related to difference between land surface and air temperatures; 2) Sensible heat flux varies linearly between hot and cold reference pixels; 3) Latent heat flux varies linearly between hot and cold reference pixels; 4) Actual ET for hot reference pixel is 0; 5) Actual ET for cold reference pixel is maximal; 6) ET can be inferred from dT, which can be estimated from land surface temperature of hot and cold reference pixels; 7) Under clear-sky conditions, actual ET will be equivalent to potential ET if land surface and air temperatures are similar (sensible heat flux is minimal).	1) No ground-based measurements required (although can be used to improve the model if local data are available); 2) No need for manual selection of hot and cold reference pixels; 3) Minimal time commitment to apply at basin scale; 4) Inexpensive (exact monetary cost not known; open-source model application for the United States being funded by the U.S. Geological Survey).	1) Does not solve for sensible or ground heat fluxes in energy balance model; 2) Does not apply land surface slope or aspect on more complicated terrain.[3]	Senay and others, 2007, 2008, 2011a, 2011b, 2013, 2016; Singh and others, 2014a, 2014b; Singh and Senay, 2016.

[1]These parameters are sourced externally to the model (inputs) or are modeled internally (outputs); other intermediate parameters not shown also are modeled internally, many more for METRIC than SSEBop.

[2]This statement may not apply to the version of METRIC being automated at larger scales using Google Earth Engine.

[3]This statement does not apply if an application of SSEBop is accounting for these two parameters when calculating dT.

accuracy is possible with the incorporation of ground-based data, no ground-based data are required. The process followed by SSEBop in estimating ET_a is relatively simple. Instantaneous or averaged surface temperature is taken from Landsat or MODIS data. Daily, weekly, or monthly air temperature is taken from Daymet data, or ground-based weather data for higher spatial resolution applications at smaller scales. A correction factor can be calculated relating land surface temperature to air temperature under clear-sky conditions for wet, vegetated pixels. A seasonally dynamic but annually static temperature difference under clear-sky conditions for each pixel is calibrated to a dry, bare pixel. Reference ET is calculated with data from gridded weather fields such as those from GDAS, or ground-based weather data for more local applications. Fractional ET is calculated using the idealized hot and cold reference values for each pixel, and estimates of ET_a at the desired time scale are calculated by multiplying reference ET by fractional ET. Although some parts of the process necessitate internal calibration, the skill required is greatly reduced.

Implementation of Large-Scale Estimation of Actual Evapotranspiration with Cloud Computing

Estimation of consumptive water use at large scales is difficult but is a key priority of the U.S. Geological Survey (USGS) and part of the focus of the National Water Census on mapping water use and availability nationally (U.S. Geological Survey, 2007; Alley and others, 2013). The USGS has been developing an objective way to estimate ET_a at this scale, but the high spatiotemporal resolution of ET_a estimates using Landsat data over large extents takes immense computing power. For example, in the two consumptive water use studies of the Colorado River Basin that used SSEBop (Singh and others, 2014a; Senay and others, 2016), 43 Landsat scenes on multiple dates, each about 1 gigabyte in size, were analyzed. The Colorado River Basin is about 7.5 percent of the area of the conterminous United States, so a continental-scale analysis of consumptive water use might need to process more than 550 scenes on multiple dates throughout the growing season. This processing involves masking clouds from the satellite images, interpolating between dates of satellite images with clear skies, and seamlessly mosaicking the satellite images. Other remote sensing data, such as air temperature, albedo, land surface elevation, and reference ET also require processing prior to inclusion in SSEBop. Because of these geospatial processing needs, an effort at this scale has not occurred.

The size of high spatial resolution satellite imagery can be prohibitive for doing large-scale analyses on an average desktop computer. For example, all the data associated with a Landsat 8 scene downloaded from Earth Explorer (https://earthexplorer.usgs.gov) are about 1 gigabyte. To download and process data for a great number of scenes on multiple dates is unfeasible at this size, particularly when exploratory analysis is first required. Cloud computing—based on computing resources that are shared over the internet—is providing an opportunity for processing an increasing amount of geospatial “big data” in a decreasing period of time (Yang and others, 2011; Lee and Kang, 2015). For example, although it might take an individual computer 10 hours to process 1 gigabyte of data, cloud computing might apportion that data among 100 (or 1,000) computers, which each take 1 hour (or 1 minute) to process its portion of the data.

Many cloud computing options, such as Amazon Web Services™, Google Earth Engine™, IBM Cloud™, or Microsoft Azure™, have potential for estimating ET_a over larger extents and longer time periods. For example, Google Earth Engine™, which uses Google’s computer infrastructure to process data in parallel on many servers, is already operative in research in the earth sciences (Yu and Gong, 2012). Google Earth Engine™ has been used to implement METRIC with automated calibration for regional-scale estimates of ET_a using Landsat data, with a beta version of a web app presented at Google’s 2015 Earth Engine™ User Summit (J.L. Huntington, Desert Research Institute, oral commun., 2016). The USGS also is using Google Earth Engine™ to implement SSEBop for estimating ET_a in the United States at a continental scale using Landsat data, with a proof-of-concept annual ET_a product showcased by the Google Earth Engine™ Team at the American Geophysical Union’s 2016 Fall Meeting (G.B. Senay, U.S. Geological Survey, written commun., 2016). Although estimates of ET_a at low spatiotemporal resolution for the contiguous United States are already available (Senay and others, 2013), higher resolution estimates are currently in development.

Summary

Water resource users and managers have a vested interest in accurately determining consumptive water use, and many approaches have been developed for measuring or estimating actual evapotranspiration (ET_a), which constitutes a large fraction of consumptive water use. The ET_a at a site can be measured directly using lysimeters, eddy covariance flux towers, or scintillometers, or indirectly using evaporation pans or Bowen ratio stations, but these direct and indirect measurements of ET_a are limited to the sites and times at which they are taken. A simple technique for estimating ET_a over larger extents and longer time periods involves the use of crop coefficients, but applying this technique more broadly is difficult because of complications with determining crop types or growth stages from aerial photography or satellite imagery. Research over many years has led to the development of remote sensing methods that are more reproducible and effective in estimating ET_a. Several remote sensing methods can be used to estimate ET_a at the high spatial resolution of agricultural fields and the large extent of river basins—a scale that is useful to water resource managers.

One of the earliest remote sensing methods for estimating ET_a was a simplified empirical regression model that estimated ET_a from the difference between land surface and air temperatures. This method for estimating ET_a is expedient because of its simplicity, and it has been applied successfully in many areas, but applications are limited by a need for site-specific parameterization that does not allow for transference to new locations. More complex analytical methods have been developed that overcome limitations of this earlier empirical method and are grounded in the theory behind the surface energy balance model, where available energy from shortwave and longwave radiation is balanced by fluxes from the heating of Earth's surface and phase changes of water such as ET_a. These methods apply an analytical approach to ET_a estimation using physically based models of varied complexity that require a combination of ground-based and remote sensing data.

This report, prepared in cooperation with the International Joint Commission, provides an overview of selected remote sensing methods used for estimating water consumed through ET_a and focuses on Mapping Evapotranspiration at High Resolution with Internalized Calibration (METRIC) and Operational Simplified Surface Energy Balance (SSEBop), two energy balance models for estimating ET_a that are currently applied successfully in the United States. The METRIC model can produce maps of ET_a at high spatial resolution (30 meters using Landsat data) for specific areas smaller than several hundred square kilometers in extent, an improvement in practice over methods used more generally at larger scales. This method has been applied for many purposes, including planning of water resources, modeling of watershed hydrology, mapping of water use by riparian vegetation, monitoring of water rights compliance, evaluation of aquifer depletion from pumpage, and assessment of irrigation performance. Similar to METRIC, SSEBop is another remote sensing method that applies the surface energy balance model to estimate ET_a, and applications of this method also have had many purposes, including drought monitoring and famine early warning in regions with sparse ground-based data, mapping of water use by different land cover classes, and estimation of ET_a in the United States at regional to continental scales. The SSEBop model has been used to produce maps of ET_a over very large extents (the conterminous United States) using lower spatial resolution (1 kilometer) Moderate Resolution Imaging Spectroradiometer (MODIS) data. Unlike METRIC, SSEBop requires less parameterization of the energy balance model, making for simpler application over larger extents, and does not have the same requirements for finely resolved ground-based data such as hourly weather information.

The METRIC and SSEBop models each have been shown to estimate ET_a with acceptable accuracies in many applications. A robust remote sensing method for estimating ET_a, METRIC has been applied successfully in the United States and internationally. The SSEBop model largely has been used to estimate ET_a in the United States. The METRIC and SSEBop models have many similarities, including their theoretical grounding in the surface energy balance model and that they can incorporate low (1 kilometer) and high (30 meter) spatial resolution data from MODIS and Landsat; however, they have important differences in data requirements, ease of implementation, and cost.

The METRIC model has shown greater accuracy at estimating ET_a than simpler techniques that use crop coefficients or vegetation indices exclusively, and also removes the need to know crop type and growth stage. The model can detect reductions in ET_a from water shortages, soil salinity, and frozen soil, and can detect evaporative losses from bare soil. In addition, many studies validating METRIC estimates of ET_a against measurements from lysimeters have shown model accuracies on daily to seasonal time scales ranging from 85 to 95 percent. The METRIC model is accurate, but the greater complexity of METRIC results in greater data requirements, and the internalized calibration of METRIC leads to greater skill required for implementation. In contrast, SSEBop is a simpler model, having reduced data requirements and greater ease of implementation without a substantial loss of accuracy in estimating ET_a. Model accuracies ranging from 80 to 95 percent on daily to annual time scales have been shown in numerous studies that validated ET_a estimates from SSEBop against eddy covariance measurements.

Estimation of consumptive water use at large scales is difficult but is a key priority of the U.S. Geological Survey (USGS) and part of the focus of the National Water Census on mapping water use and availability nationally. The USGS has been developing an objective way to estimate ET_a at this scale, but the high spatiotemporal resolution of ET_a estimates using Landsat data over large extents takes immense computing power. Cloud computing is providing an opportunity for processing an increasing amount of geospatial "big data" in a decreasing period of time. For example, Google Earth Engine™ has been used to implement METRIC with automated calibration for regional-scale estimates of ET_a using Landsat data. The USGS also is using Google Earth Engine™ to implement SSEBop for estimating ET_a in the United States at a continental scale using Landsat data. Although estimates of ET_a at low spatiotemporal resolution for the contiguous United States are already available, higher resolution estimates are currently in development.

Acknowledgments

We thank Sean Lawlor and Dr. Gabriel Senay for providing reviews that helped improve this report.

References Cited

Allen, R.G., 2000, Using the FAO-56 dual crop coefficient method over an irrigated region as part of an evapotranspiration intercomparison study: Journal of Hydrology, v. 229, no. 1–2, p. 27–41. [Also available at https://doi.org/10.1016/S0022-1694(99)00194-8.]

Allen, R.G., Burnett, B., Kramber, W., Huntington, J., Kjaersgaard, J., Kilic, A., Kelly, C., and Trezza, R., 2013, Automated calibration of the METRIC-Landsat Evapotranspiration Process: Journal of the American Water Resources Association, v. 49, no. 3, p. 563–576. [Also available at http://dx.doi.org/10.1111/jawr.12056.]

Allen, R.G., Irmak, A., Trezza, R., Hendrickx, J.M.H., Bastiaanssen, W., and Kjaersgaard, J., 2011a, Satellite-based ET estimation in agriculture using SEBAL and METRIC: Hydrological Processes, v. 25, no. 26, p. 4011–4027. [Also available at http://dx.doi.org/10.1002/hyp.8408.]

Allen, R.G., Pereira, L.S., Howell, T.A., and Jensen, M.E., 2011b, Evapotranspiration information reporting—I. Factors governing measurement accuracy: Agricultural Water Management, v. 98, no. 6, p. 899–920. [Also available at https://doi.org/10.1016/j.agwat.2010.12.015.]

Allen, R.G., Pereira, L., Raes, D., and Smith, M., 1998, Crop evapotranspiration—Guidelines for computing crop water requirements: Food and Agriculture Organization of the United Nations Irrigation and Drainage Paper 56. [Also available at http://www.fao.org/docrep/X0490E/X0490E00.htm.]

Allen, R.G., Pereira, L.S., Smith, M., Raes, D., and Wright, J.L., 2005a, FAO-56 dual crop coefficient method for estimating evaporation from soil and application extensions: Journal of Irrigation and Drainage Engineering, v. 131, no. 1, p. 2–13. [Also available at https://doi.org/10.1061/(ASCE)0733-9437(2005)131:1(2).]

Allen, R.G., Tasumi, M., Morse, A., and Trezza, R., 2005b, A Landsat-based energy balance and evapotranspiration model in Western US water rights regulation and planning: Irrigation and Drainage Systems, v. 19, no. 3, p. 251–268. [Also available at http://dx.doi.org/10.1007/s10795-005-5187-z.]

Allen, R.G., Tasumi, M., Morse, A., Trezza, R., Wright, J.L., Bastiaanssen, W., Kramber, W., Lorite, I., and Robison, C.W., 2007a, Satellite-based energy balance for Mapping Evapotranspiration with Internalized Calibration (METRIC)—Applications: Journal of Irrigation and Drainage Engineering, v. 133, no. 4, p. 395–406. [Also available at https://doi.org/10.1061/(ASCE)0733-9437(2007)133:4(395).]

Allen, R.G., Tasumi, M., and Trezza, R., 2007b, Satellite-based energy balance for Mapping Evapotranspiration with Internalized Calibration (METRIC)—Model: Journal of Irrigation and Drainage Engineering, v. 133, no. 4, p. 380–394. [Also available at https://doi.org/10.1061/(ASCE)0733-9437(2007)133:4(380).]

Alley, W.M., Evenson, E.J., Barber, N.L., Bruce, B.W., Dennehy, K.F., Freeman, M.C., Freeman, W.O., Fischer, J.M., Hughes, W.B., Kennen, J.G., Kiang, J.E., Maloney, K.O., Musgrove, M., Ralston, B., Tessler, S., and Verdin, J.P., 2013, Progress toward establishing a national assessment of water availability and use: U.S. Geological Survey Circular 1384, 34 p.. [Also available at http://pubs.usgs.gov/circ/1384.]

American Society of Civil Engineers, 2005, The ASCE standardized reference evapotranspiration equation: Environmental and Water Resources Institute of the American Society of Civil Engineers Task Committee on Standardization of Reference Evapotranspiration Final Report, 216 p.

Anderson, M.C., Norman, J.M., Diak, G.R., Kustas, W.P., and Mecikalski, J.R., 1997, A two-source time-integrated model for estimating surface fluxes using thermal infrared remote sensing: Remote Sensing of Environment, v. 60, no. 2, p. 195–216. [Also available at https://doi.org/10.1016/S0034-4257(96)00215-5.]

Bastiaanssen, W.G.M., 1995, Regionalization of surface flux densities and moisture indicators in composite terrain—A remote sensing approach under clear skies in Mediterranean climates: Wageningen, The Netherlands, Wageningen University, Ph.D. dissertation.

Bastiaanssen, W.G.M., 2000, SEBAL-based sensible and latent heat fluxes in the irrigated Gediz Basin, Turkey: Journal of Hydrology, v. 229, no. 1–2, p. 87–100. [Also available at https://doi.org/10.1016/S0022-1694(99)00202-4.]

Bastiaanssen, W.G.M., Menenti, M., Feddes, R.A., and Holtslag, A.A.M., 1998a, A remote sensing surface energy balance algorithm for land (SEBAL)—1. Formulation: Journal of Hydrology, v. 212–213, p. 198–212. [Also available at https://doi.org/10.1016/S0022-1694(98)00253-4.]

Bastiaanssen, W.G.M., Noordman, E., Pelgrum, H., Davids, G., Thoreson, B., and Allen, R., 2005, SEBAL model with remotely sensed data to improve water-resources management under actual field conditions: Journal of Irrigation and Drainage Engineering, v. 131, no. 1, p. 85–93. [Also available at https://doi.org/10.1061/(ASCE)0733-9437(2005)131:1(85).]

Bastiaanssen, W.G.M., Pelgrum, H., Wang, J., Ma, Y., Moreno, J.F., Roerink, G.J., and van der Wal, T., 1998b, A remote sensing surface energy balance algorithm for land (SEBAL)—Part 2. Validation: Journal of Hydrology, v. 212–213, p. 213–229. [Also available at https://doi.org/10.1016/S0022-1694(98)00254-6.]

Biggs, T.W., Petropoulos, G.P., Velpuri, N.M., Marshall, M., Glenn, E.P., Nagler, P., and Messina, A., 2015, Remote sensing of actual evapotranspiration from cropland, chap. 3 of Thenkabail, P.S., ed., Remote sensing of water resources, disasters, and urban studies: CRC Press, p. 59–99. [Also available at https://pubs.er.usgs.gov/publication/70176490.]

Carlson, T.N., and Buffum, M.J., 1989, On estimating total daily evapotranspiration from remote surface temperature measurements: Remote Sensing of Environment, v. 29, no. 2, p. 197–207. [Also available at https://doi.org/10.1016/0034-4257(89)90027-8.]

Carr, J.E., Chase, E.B., Paulson, R.W., and Moody, D.W., 1990, National water summary 1987—Hydrologic events and water supply and use: U.S. Geological Survey Water Supply Paper 2350, 567 p.. [Also available at http://pubs.er.usgs.gov/publication/wsp2350.]

Chen, M., Senay, G.B., Singh, R.K., and Verdin, J.P., 2016, Uncertainty analysis of the Operational Simplified Surface Energy Balance (SSEBop) model at multiple flux tower sites: Journal of Hydrology, v. 536, p. 384–399. [Also available at https://doi.org/10.1016/j.jhydrol.2016.02.026.]

Choudhury, B.J., Ahmed, N.U., Idso, S.B., Reginato, R.J., and Daughtry, C.S.T., 1994, Relations between evaporation coefficients and vegetation indices studied by model simulations: Remote Sensing of Environment, v. 50, no. 1, p. 1–17. [Also available at https://doi.org/10.1016/0034-4257(94)90090-6.]

French, A.N., Hunsaker, D.J., and Thorp, K.R., 2015, Remote sensing of evapotranspiration over cotton using the TSEB and METRIC energy balance models: Remote Sensing of Environment, v. 158, p. 281–294. [Also available at https://doi.org/10.1016/j.rse.2014.11.003.]

Fritschen, L.J., 1965, Accuracy of evapotranspiration determinations by the Bowen ratio method: Hydrological Sciences Journal, v. 10, no. 2, p. 38–48. [Also available at http://dx.doi.org/10.1080/02626666509493388.]

Gowda, P.H., Chavez, J.L., Colaizzi, P.D., Evett, S.R., Howell, T.A., and Tolk, J.A., 2008a, ET mapping for agricultural water management—Present status and challenges: Irrigation Science, v. 26, no. 3, p. 223–237. [Also available at http://dx.doi.org/10.1007/s00271-007-0088-6.]

Gowda, P.H., Chávez, J.L., Howell, T.A., Marek, T.H., and New, L.L., 2008b, Surface energy balance based evapotranspiration mapping in the Texas High Plains: Sensors, v. 8, no. 8, p. 5186–5201. [Also available at http://dx.doi.org/10.3390/s8085186.]

Gowda, P.H., Senay, G.B., Howell, T.A., and Marek, T.H., 2009, Lysimetric evaluation of simplified surface energy balance approach in the Texas High Plains: Applied Engineering in Agriculture, v. 25, no. 5, p. 665–669. [Also available at https://pubs.er.usgs.gov/publication/70043493.]

Helsel, D.R., and Hirsch, R.M., 2002, Statistical methods in water resources: U.S. Geological Survey Techniques of Water-Resources Investigations, book 4, chap. A3, 522 p. [Also available at http://water.usgs.gov/pubs/twri/twri4a3.]

Idso, S.B., Schmugge, T.J., Jackson, R.D., and Reginato, R.J., 1975, The utility of surface temperature measurements for the remote sensing of surface soil water status: Journal of Geophysical Research, v. 80, no. 21, p. 3044–3049. [Also available at http://dx.doi.org/10.1029/JC080i021p03044.]

Jackson, R.D., Reginato, R.J., and Idso, S.B., 1977, Wheat canopy temperature—A practical tool for evaluating water requirements: Water Resources Research, v. 13, no. 3, p. 651–656. [Also available at http://dx.doi.org/10.1029/WR013i003p00651.]

Khan, S.I., Chang, N.-B., Hong, Y., Xue, X., and Zhang, Y., 2015, Remote sensing technologies for multiscale hydrological studies—Advances and perspectives, chap. 1 of Thenkabail, P.S., ed., Remote sensing of water resources, disasters, and urban studies: CRC Press, p. 3–21. [Also available at https://pubs.er.usgs.gov/publication/70176490.]

Lee, J.-G., and Kang, M., 2015, Geospatial big data—Challenges and opportunities: Big Data Research, v. 2, no. 2, p. 74–81. [Also available at https://doi.org/10.1016/j.bdr.2015.01.003.]

Li, Z.-L., Tang, R., Wan, Z., Bi, Y., Zhou, C., Tang, B., Yan, G., and Zhang, X., 2009, A review of current methodologies for regional evapotranspiration estimation from remotely sensed data: Sensors, v. 9, no. 5, p. 3801–3853. [Also available at http://dx.doi.org/10.3390/s90503801.]

Liou, Y.-A., and Kar, S.K., 2014, Evapotranspiration estimation with remote sensing and various surface energy balance algorithms—A review: Energies, v. 7, no. 5, p. 2821–2849. [Also available at http://dx.doi.org/10.3390/en7052821.]

Long, D., and Singh, V.P., 2013, Assessing the impact of end-member selection on the accuracy of satellite-based spatial variability models for actual evapotranspiration estimation: Water Resources Research, v. 49, no. 5, p. 2601–2618. [Also available at http://dx.doi.org/10.1002/wrcr.20208.]

Maupin, M.A., Kenny, J.F., Hutson, S.S., Lovelace, J.K., Barber, N.L., and Linsey, K.S., 2014, Estimated use of water in the United States in 2010: U.S. Geological Survey Circular 1405, 56 p.. [Also available at http://pubs.usgs.gov/circ/1405.]

Mecikalski, J.R., Diak, G.R., Anderson, M.C., and Norman, J.M., 1999, Estimating fluxes on continental scales using remotely sensed data in an Atmospheric–Land Exchange Model: Journal of Applied Meteorology, v. 38, no. 9, p. 1352–1369. [Also available at https://doi.org/10.1175/1520-0450(1999)038%3C1352:EFOCSU%3E2.0.CO;2.]

Meijninger, W.M.L., Green, A.E., Hartogensis, O.K., Kohsiek, W., Hoedjes, J.C.B., Zuurbier, R.M., and De Bruin, H.A.R., 2002, Determination of area-averaged water vapour fluxes with large aperture and radio wave scintillometers over a heterogeneous surface—Flevoland field experiment: Boundary-Layer Meteorology, v. 105, no. 1, p. 63–83. [Also available at http://dx.doi.org/10.1023/A:1019683616097.]

Morton, C.G., Huntington, J.L., Pohll, G.M., Allen, R.G., McGwire, K.C., and Bassett, S.D., 2013, Assessing calibration uncertainty and automation for estimating evapotranspiration from agricultural areas using METRIC: Journal of the American Water Resources Association, v. 49, no. 3, p. 549–562. [Also available at http://dx.doi.org/10.1111/jawr.12054.]

Mu, Q., Heinsch, F.A., Zhao, M., and Running, S.W., 2007, Development of a global evapotranspiration algorithm based on MODIS and global meteorology data: Remote Sensing of Environment, v. 111, no. 4, p. 519–536. [Also available at https://doi.org/10.1016/j.rse.2007.04.015.]

Nash, J.E., and Sutcliffe, J.V., 1970, River flow forecasting through conceptual models—Part 1. A discussion of principles: Journal of Hydrology, v. 10, no. 3, p. 282–290. [Also available at https://doi.org/10.1016/0022-1694(70)90255-6.]

Nieuwenhuis, G.J.A., Smidt, E.H., and Thunnissen, H.A.M., 1985, Estimation of regional evapotranspiration of arable crops from thermal infrared images: International Journal of Remote Sensing, v. 6, no. 8, p. 1319–1334. [Also available at http://www.tandfonline.com/doi/abs/10.1080/01431168508948282.]

Norman, J.M., Kustas, W.P., and Humes, K.S., 1995, Source approach for estimating soil and vegetation energy fluxes in observations of directional radiometric surface temperature: Agricultural and Forest Meteorology, v. 77, no. 3–4, p. 263–293. [Also available at https://doi.org/10.1016/0168-1923(95)02265-Y.]

Norman, J.M., Kustas, W.P., Prueger, J.H., and Diak, G.R., 2000, Surface flux estimation using radiometric temperature—A dual-temperature-difference method to minimize measurement errors: Water Resources Research, v. 36, no. 8, p. 2263–2274. [Also available at http://dx.doi.org/10.1029/2000WR900033.]

Pruitt, W.O., and Angus, D.E., 1960, Large weighing lysimeter for measuring evapotranspiration: Transactions of the ASABE, v. 3, no. 2, p. 13–15. [Also available at http://dx.doi.org/10.13031/2013.41105.]

Qiu, G.Y., Yano, T., and Momii, K., 1998, An improved methodology to measure evaporation from bare soil based on comparison of surface temperature with a dry soil surface: Journal of Hydrology, v. 210, no. 1–4, p. 93–105. [Also available at https://doi.org/10.1016/S0022-1694(98)00174-7.]

Roerink, G.J., Su, Z., and Menenti, M., 2000, S-SEBI—A simple remote sensing algorithm to estimate the surface energy balance: Physics and Chemistry of the Earth, Part B: Hydrology, Oceans and Atmosphere, v. 25, no. 2, p. 147–157. [Also available at https://doi.org/10.1016/S1464-1909(99)00128-8.]

Ruhoff, A.L., Paz, A.R., Collischonn, W., Aragao, L.E.O.C., Rocha, H.R., and Malhi, Y.S., 2012, A MODIS-based energy balance to estimate evapotranspiration for clear-sky days in Brazilian tropical savannas: Remote Sensing, v. 4, no. 3, p. 703–725. [Also available at http://dx.doi.org/10.3390/rs4030703.]

Santos, C., Lorite, I.J., Tasumi, M., Allen, R.G., and Fereres, E., 2008, Integrating satellite-based evapotranspiration with simulation models for irrigation management at the scheme level: Irrigation Science, v. 26, no. 3, p. 277–288. [Also available at http://dx.doi.org/10.1007/s00271-007-0093-9.]

Seguin, B., Courault, D., and Guérif, M., 1994, Surface temperature and evapotranspiration—Application of local scale methods to regional scales using satellite data: Remote Sensing of Environment, v. 49, no. 3, p. 287–295. [Also available at https://doi.org/10.1016/0034-4257(94)90023-X.]

Seguin, B., and Itier, B., 1983, Using midday surface temperature to estimate daily evaporation from satellite thermal IR data: International Journal of Remote Sensing, v. 4, no. 2, p. 371–383. [Also available at http://dx.doi.org/10.1080/01431168308948554.]

Senay, G.B., Bohms, S., Singh, R.K., Gowda, P.H., Velpuri, N.M., Alemu, H., and Verdin, J.P., 2013, Operational evapotranspiration mapping using remote sensing and weather datasets—A new parameterization for the SSEB approach: Journal of the American Water Resources Association, v. 49, no. 3, p. 577–591. [Also available at http://dx.doi.org/10.1111/jawr.12057.]

Senay, G.B., Budde, M.E., and Verdin, J.P., 2011a, Enhancing the Simplified Surface Energy Balance (SSEB) approach for estimating landscape ET—Validation with the METRIC model: Agricultural Water Management, v. 98, no. 4, p. 606–618. [Also available at https://doi.org/10.1016/j.agwat.2010.10.014.]

Senay, G.B., Budde, M., Verdin, J.P., and Melesse, A.M., 2007, A coupled remote sensing and simplified surface energy balance approach to estimate actual evapotranspiration from irrigated fields: Sensors, v. 7, no. 6, p. 979–1000. [Also available at http://dx.doi.org/10.3390/s7060979.]

Senay, G.B., Friedrichs, M., Singh, R.K., and Velpuri, N.M., 2016, Evaluating Landsat 8 evapotranspiration for water use mapping in the Colorado River Basin: Remote Sensing of Environment, v. 185, p. 171–185. [Also available at https://doi.org/10.1016/j.rse.2015.12.043.]

Senay, G.B., Leake, S., Nagler, P.L., Artan, G., Dickinson, J., Cordova, J.T., and Glenn, E.P., 2011b, Estimating basin scale evapotranspiration (ET) by water balance and remote sensing methods: Hydrological Processes, v. 25, no. 26, p. 4037–4049. [Also available at http://dx.doi.org/10.1002/hyp.8379.]

Senay, G.B., Verdin, J.P., Lietzow, R., and Melesse, A.M., 2008, Global daily reference evapotranspiration modeling and evaluation: Journal of the American Water Resources Association, v. 44, no. 4, p. 969–979. [Also available at http://dx.doi.org/10.1111/j.1752-1688.2008.00195.x.]

Singh, R.K., and Senay, G.B., 2016, Comparison of four different energy balance models for estimating evapotranspiration in the Midwestern United States: Water, v. 8, no. 1, 9 p.. [Also available at http://dx.doi.org/10.3390/w8010009.]

Singh, R.K., Senay, G.B., Velpuri, N.M., Bohms, S., Scott, R.L., and Verdin, J.P., 2014a, Actual evapotranspiration (water use) assessment of the Colorado River Basin at the Landsat resolution using the Operational Simplified Surface Energy Balance Model: Remote Sensing, v. 6, no. 1, p. 233–256. [Also available at https://doi.org/10.3390/rs6010233.]

Singh, R.K., Senay, G.B., Velpuri, N.M., Bohms, S., and Verdin, J.P., 2014b, On the downscaling of actual evapotranspiration maps based on combination of MODIS and Landsat-based actual evapotranspiration estimates: Remote Sensing, v. 6, no. 11, p. 10483–10509. [Also available at http://dx.doi.org/10.3390/rs61110483.]

Snyder, R.L., 1992, Equation for evaporation pan to evapotranspiration conversions: Journal of Irrigation and Drainage Engineering, v. 118, no. 6, p. 977–980. [Also available at https://doi.org/10.1061/(ASCE)0733-9437(1992)118:6(977).]

Su, Z., 2002, The Surface Energy Balance System (SEBS) for estimation of turbulent heat fluxes: Hydrology and Earth System Sciences, v. 6, no. 1, p. 85–100. [Also available at http://dx.doi.org/10.5194/hess-6-85-2002.]

Swinbank, W.C., 1951, The measurement of vertical transfer of heat and water vapor by eddies in the lower atmosphere: Journal of Meteorology, v. 8, no. 3, p. 135–145. [Also available at https://doi.org/10.1175/1520-0469(1951)008%3C0135:TMOVTO%3E2.0.CO;2.]

Taconet, O., Carlson, T., Bernard, R., and Vidal-Madjar, D., 1986, Evaluation of a surface/vegetation parameterization using satellite measurements of surface temperature: Journal of Climate and Applied Meteorology, v. 25, no. 11, p. 1752–1767. [Also available at https://doi.org/10.1175/1520-0450(1986)025%3C1752:EOASPU%3E2.0.CO;2.]

Tasumi, M., 2003, Progress in operational estimation of regional evapotranspiration using satellite imagery: Moscow, Idaho, University of Idaho, Ph.D. dissertation.

Tasumi, M., Allen, R.G., Trezza, R., and Wright, J.L., 2005a, Satellite-based energy balance to assess within-population variance of crop coefficient curves: Journal of Irrigation and Drainage Engineering, v. 131, no. 1, p. 94–109. [Also available at https://doi.org/10.1061/(ASCE)0733-9437(2005)131:1(94).]

Tasumi, M., Trezza, R., Allen, R.G., and Wright, J.L., 2005b, Operational aspects of satellite-based energy balance models for irrigated crops in the semi-arid U.S.: Irrigation and Drainage Systems, v. 19, no. 3–4, p. 355–376. [Also available at http://dx.doi.org/10.1007/s10795-005-8138-9.]

Thornton, P.E., Running, S.W., and White, M.A., 1997, Generating surfaces of daily meteorological variables over large regions of complex terrain: Journal of Hydrology, v. 190, no. 3–4, p. 214–251. [Also available at https://doi.org/10.1016/S0022-1694(96)03128-9.]

Timmermans, W.J., Kustas, W.P., Anderson, M.C., and French, A.N., 2007, An intercomparison of the Surface Energy Balance Algorithm for Land (SEBAL) and the Two-Source Energy Balance (TSEB) modeling schemes: Remote Sensing of Environment, v. 108, no. 4, p. 369–384. [Also available at https://doi.org/10.1016/j.rse.2006.11.028.]

Trezza, R., Allen, R.G., and Tasumi, M., 2013, Estimation of actual evapotranspiration along the Middle Rio Grande of New Mexico using MODIS and Landsat imagery with the METRIC model: Remote Sensing, v. 5, no. 10, p. 5397–5423. [Also available at http://dx.doi.org/10.3390/rs5105397.]

U.S. Geological Survey, 2007, Facing tomorrow's challenges—U.S. Geological Survey science in the decade 2007–2017: U.S. Geological Survey Circular 1309, 70 p.. [Also available at https://pubs.usgs.gov/circ/2007/1309.]

Vörösmarty, C.J., Green, P., Salisbury, J., and Lammers, R.B., 2000, Global water resources—Vulnerability from climate change and population growth: Science, v. 289, no. 5477, p. 284–288. [Also available at http://dx.doi.org/10.1126/science.289.5477.284.]

Yang, C., Goodchild, M., Huang, Q., Nebert, D., Raskin, R., Xu, Y., Bambacus, M., and Fay, D., 2011, Spatial cloud computing—How can the geospatial sciences use and help shape cloud computing?: International Journal of Digital Earth, v. 4, no. 4, p. 305–329. [Also available at http://dx.doi.org/10.1080/17538947.2011.587547.]

Yang, Y., Shang, S., and Jiang, L., 2012, Remote sensing temporal and spatial patterns of evapotranspiration and the responses to water management in a large irrigation district of North China: Agricultural and Forest Meteorology, v. 164, p. 112–122. [Also available at https://doi.org/10.1016/j.agrformet.2012.05.011.]

Yang, Y., Su, H., Zhang, R., Tian, J., and Li, L., 2015, An enhanced two-source evapotranspiration model for land (ETEML)—Algorithm and evaluation: Remote Sensing of Environment, v. 168, p. 54–65. [Also available at https://doi.org/10.1016/j.rse.2015.06.020.]

Yu, L., and Gong, P., 2012, Google Earth as a virtual globe tool for Earth science applications at the global scale—Progress and perspectives: International Journal of Remote Sensing, v. 33, no. 12, p. 3966–3986. [Also available at http://dx.doi.org/10.1080/01431161.2011.636081.]

For additional information concerning this publication, contact:
Director, USGS Wyoming-Montana Water Science Center
3162 Bozeman Avenue
Helena, MT 59601
(406) 457–5900

Or visit the Wyoming-Montana Water Science Center website at:
https://wy-mt.water.usgs.gov

Publishing support provided by:
Rolla Publishing Service Center

McShane and others—**Models for Estimating Actual Evapotranspiration with Remote Sensing at High Spatiotemporal Resolution**—SIR 2017–5087

ISSN 2328-0328 (online)
https://doi.org/10.3133/sir20175087